Mem. S.A.It. Vol. 90, 663

Memorie della

Implications of non-standard physics on the future evolution of exoplanets orbiting red giant stars

S. Arceo Díaz[1], E. E. Bricio Barrios[1], K. Zuber[2], J. M. González Perez[1], and J. A. Verduzco Ramirez[1]

[1] Tecnológico Nacional de México/Instituto Tecnológico de Colima - Amado Nervo, Villa de Álvarez, 28979 Colima, Mexico, e-mail: elena.bricio@itcolima.edu.mx

[2] Institute of Nuclear and Particle Physics, Technische Universität Dresden, Zellescher Weg 19, 01069 Dresden, Germany

Abstract. We discuss the implications on the future evolution of planetary systems orbiting red giant stars, if physical reactions involving the production of axions and the enhanced decay of plasmons into neutrinos, as a consequence of neutrinos having a magnetic dipole moment, are assumed to be happening simultaneously within the stellar core. Simulations were created by employing a numerical code to calculate the physical properties of stellar models from the main sequence to the end of the red giant phase, for stars with a mass range between 0.9 and 1.9 $M_\odot$ and we analyze the most noticeable differences to canonical stellar evolution. Two exoplanet systems, known for harboring single red giant stars, were modelled by using the predicted stellar properties to calculate the temporal variation of the habitable zone and the orbital distance.

Key words. Stars: red giants – Stars: stellar simulation – Stars: neutrino cooling – Particles: axions

1. Introduction

Currently, there are 4031 confirmed exoplanets within the NASA Exoplanet Archive[1]. Although the majority of the known exoplanets orbit around main sequence (MS) stars, 154 red giant systems have already been identified (Jiang & Zhu 2018). This increment in the number of observational evidence of planets orbiting evolved low-mass stars could not only help to improve our understanding on the fate of these planets once their parent star has left the MS but, also, to provide a testing ground for physical theories beyond the standard model.

One of the classical astrophysical scenarios is the future of our own solar system once the Sun becomes a red giant. Recent works (Schröder & Smith 2008; Ramírez & Kaltenegger 2016) conclude that Earth (along with the innermost terrestrial planets) will be engulfed by the red giant Sun and relate this fate to the physical processes affecting the stellar envelope. However, energy dissipation, caused by the production of low-mass particles directly from the stellar core, can play a ma-

[1] https://exoplanets.nasa.gov/exoplanet-catalog/

jor role in defining the stellar bolometric luminosity and radius prior to the helium flash: energy dissipation delays helium ignition, which terminates the red giant branch (RGB) phase, allowing more time for the star to become brighter and larger (as the hydrogen burning shell surrounding the degenerate helium core has to accelerate hydrogen fusion to maintain itself against the gravitational pull of the core).

In a recent work (Arceo-Díaz et al. 2019), the survival of Earth to the RGB and asymptotic giant branch (AGB) phases of the Sun was revisited, considering a scenario in which both two non-standard physical phenomena remained active within the solar core since the beginning of the MS: axion production by the Compton reaction and, during phases in which electron degeneracy becomes increasingly important, the Bremmstrahhlung reaction (Raffelt & Weiss 1995) and the enhanced emission rate of neutrinos trough plasmon decay (Raffelt & Weiss 1992). The main result was a delay in the termination of both giant phases that allowed the star to become about 30% brighter, considerably affecting the habitable zone, and larger, $76R_{\odot}$ at the tip of the RGB (TRGB) and $58R_{\odot}$ at the tip of the AGB. These changes make impossible for Earth, Venus and Mercury to escape and become engulfed in a shorter time than in the canonical scenario and shortens the time that (the fleeing) Mars expends on the habitable zone.

In this work, we discuss the implications of these non-standard ingredients on the physical properties of stars within a wider range of metallicity and mass and use stellar models to analyze if two exoplanets, orbiting the largest known low-mass red giants, could survive to their RGB phase.

2. Methodology

Our study uses the stellar evolution code created by Eggleton (Eggleton 1971) as its computational basis. The present version calculates the enhanced energy cooling caused by plasmon decay into neutrinos and axion emission with the formulae proposed by Haft et al. (1994) and Raffelt & Weiss (1995) (the cooling caused by the other thermal reactions producing neutrino pairs was calculated from numerical tables following the prescriptions discussed in Itoh et al. 1992 and Itoh et al. 1996). As for the values of the magnetic dipole moment of neutrinos and the axion-electron coupling constant, we adopt the values proposed by Arceo-Díaz et al. (2015a; 2015b), which are based on the evidence found by analyzing the TRGB of omega Centauri and 24 other galactic globular clusters: $\alpha_{\rm a} = 0.5 \times 10^{-26}$, $\mu_{\nu} = 2.2 \times 10^{-12} \mu_{\rm B}$.

To measure the effects of non-standard energy losses, we constructed stellar tracks with the following initial values: M_i=0.9, 1.4, 1.9 $M_{\odot}$ (covering the mass range in which the physical conditions within the degenerate core of a red giant make plasmon decay the main channel for energy cooling). Three sets of models, having the initial metallicity of Z=0.001, 0.01 and 0.02 and hydrogen and helium mass fractions according to the prescription defined by Pols et al. (1995). For each track, we defined the theoretical TRGB as the model in which helium luminosity reaches 10 $L_{\odot}$. Between this point and the true helium flash, bolometric luminosity does not varies much and, as long as the canonical and non-standard models have the same helium luminosity, its increment due to non-standard physics is not affected by this choice.

The mass-loss rate occurring during the red giant phase follows the empirical formula by Schröder & Cuntz (2005). Mass-loss depends on the chromospheric flux of mechanical energy and is related to the surface gravity, bolometric luminosity and effective temperature. As non-standard energy losses affect these parameters, the mass-loss rate parameter had to be reduced to a 58% to ensure that the TRGB mass on non-standard models is the same as the canonical models.

Once the TRGB models were calculated we analyzed the main differences on the physical properties of canonical and non-standard stellar evolution. To provide examples of what would be the consequences for a planet orbiting a red giant with non-standard properties, two stellar system harbouring red giants (HD 220074 and HD 158996) were chosen as examples. The radius of the habitable zone, in terms of stellar luminosity, was calculated by

Table 1. TRGB models for low-mass stars.

	$M_* = 0.9M_\odot$					
	Z=0.001		Z=0.01		Z=0.02	
	Canonical	Non-std.	Canonical	Non-std.	Canonical	Non-std.
$M_*[M_\odot]$	0.703	0.703	0.572	0.572	0.509	0.509
$M_c[M_\odot]$	0.491	0.524	0.480	0.507	0.473	0.497
$L_{bol}[L_\odot]$	2208	3226	2559	3471	2574	3392
$R_*[R_\odot]$	105	136	171	201	182	176
	$M_i = 1.4M_\odot$					
	Z=0.001		Z=0.01		Z=0.02	
	Canonical	Non-std.	Canonical	Non-std.	Canonical	Non-std.
$M_*[M_\odot]$	1.320	1.321	1.294	1.299	1.291	1.297
$M_c[M_\odot]$	0.483	0.519	0.478	0.505	0.472	0.496
$L_{bol}[L_\odot]$	2056	3182	2564	3530	2636	3538
$R_*[R_\odot]$	88	118	143	181	164	211
	$M_i = 1.9M_\odot$					
	Z=0.001		Z=0.01		Z=0.02	
	Canonical	Non-std.	Canonical	Non-std.	Canonical	Non-std.
$M_*[M_\odot]$	1.8593	1.552	1.8495	1.8476	1.8496	1.8487
$M_c[M_\odot]$	0.470	0.518	0.466	0.502	0.462	0.494
$L_{bol}[L_\odot]$	1721	3099	2206	3424	2318	3449
$R_*[R_\odot]$	72	107	114	158	133	186

using the formula by Whitmire & Reynolds (1996). The orbital distance between each exoplanet and its star and the loss of orbital angular momentum due to tidal drag were calculated, using the formula by Zahn (1973), with a fourth-order Runge-Kutta algorithm that uses the physical properties of the stellar model and the current calibrations for orbital parameters of each system as its input.

3. Results

3.1. Generic stellar models

The TRGB models for our stellar tracks are shown in Table 1: each of the three sub-tables contains three pairs of TRGB models (labeled as "canonical" and "non-standard") with Z=0.001, 0.01 and 0.02 and the same initial mass (M_i=0.9, 1.4 or 1.9 $M_\odot$). Each row shows the total stellar and core mass, the bolometric luminosity, the radius and the effective temperature just before the helium flash, quantified in solar units and Kelvins, respectively. As can be seen, the TRGB mass of non-standard models shows the difference of less than 0.01 $M_\odot$ with respect to their canonical analogs (this is a consequence of reducing the value of the mass-loss parameter in the prescription by Schröder & Cuntz (2005) for non-dust-driven mass-loss, considering that non-standard models should not contradict the current observational calibrations on the mass of red giants).

Independently on initial mass or metallicity, the non-standard models of Table 1 show larger core masses and, as a consequence on its dependence on this parameter, a larger bolometric luminosity than canonical models (this difference is more prominent for models with an increasing initial mass, going from 0.033 to 0.048 $M_\odot$ for the models with M_i = 0.9 to M_i = 1.9 $M_\odot$, all with Z = 0.001). This increment in core mass is a direct result on the extra time that the model needs to expend to reach favorable conditions for the helium flash to occur and the enhanced burning rate of the hydrogen shell to compensate the gravitational pull of an increasingly more massive degenerate core (see Fig. 2 in Arceo-Díaz et al. 2019). Also, one can notice that the non-standard increment in core mass is smaller for the models with higher metallicity: the non-standard increment for the TRGB models with Z = 0.02 is only 66% of the increment for models with Z = 0.001. This could be a consequence of the fact that the initial hydrogen mass fraction was calculated by following Pols et al. (1995), which makes low-metallicity models to have more hydrogen accessible for the burning shell during the red giant phase. In all cases, the increment in core mass results in a larger TRGB luminosity, with increments that go up to $\sim$1300 $L_\odot$, which could have a considerable impact on the habitable zone by moving it outwards (see below).

Another important effect caused by the enhanced cooling of the stellar core is that the increment in the stellar radius, during the red giant phase, grows proportionally to the initial mass and metallicity, going up to $\sim$50 $R_\odot$ for the model with M_i=1.9 $M_\odot$ and Z=0.02. This is a direct result of the accelerated expansion rate that the stellar envelope undergoes as the hydrogen-burning shell compensates the cooling of the stellar core and it has a large impact on defining the fate of exoplanets orbiting red giant stars.

To illustrate how this changes could affect the survival of exoplanets orbiting stars that are going trough the RGB phase, two stellar systems were modelled: HD 220074 and HD 158996. Both systems are listed within the NASA exoplanet database as those with the largest red giants and, at least, one hot Jupiter.

3.2. HD 220074

The observational calibrations for the stellar properties and orbital parameters for HD 220074 were taken from Lee et al. (2013). The star of this system has a stellar radius $R_* = 49.7 \pm 9.5$ $R_\odot$, an estimated stellar mass $M_* = 1.2 \pm 0.3$ $M_\odot$ and an effective temperature $T_{\rm eff} = 3935 \pm 110$ K. Around this star, an exoplanet with an estimated mass $M_p = 11$ $M_{\rm jup}$ is orbiting at an average distance $R_{\rm orb} = 1.6$ au (from these values, the estimated orbital angular momentum is $\Lambda = 1.3858 \times 10^{44}$ kg m^2 s^{-1}). These values were used to calculate a stellar model that could fit within the error bars for stellar radius and temperature. Table 2 shows the best fitting model and the canonical and non-standard TRGB models (that differentiate themselves until they are very close to the helium flash). As with the models shown in Table 1, the non-standard models are almost a 900 $L_\odot$ brighter and larger by $\sim$50 $R_\odot$. The left panel in Figure 1 shows the temporal evolution for stellar radius, orbital distance and the upper and lower limits of the habitable zone for HD 220074. In both scenarios, the loss of orbital angular momentum by tidal drag is strong enough to pull the planet towards its parent star, although in the non-standard scenario this happens almost 30 million years earlier. On the other side, there are no visible effects on the limit of the habitable zone until the very end of the red giant phase (thus, this would only affect any planet located at a larger distance).

3.3. HD 158996

The observational calibrations for the stellar properties and orbital parameters for HD 158996 were taken from Bang et al. (2018). The star of this system has $R_* = 50.3 \pm 4.3$ $R_\odot$, $M_* = 1.8 \pm 0.3$ $M_\odot$ and $T_{\rm eff} = 4069 \pm 30$ K. According to that same reference, the host planet orbits this star at $R_{\rm orb} = 2.1$ au, with $\Lambda = 2.3023 \times 10^{44}$ kg m^2 s^{-1}, and has a mass of $M_p = 14$ $M_{\rm jup}$. Our best fitting model for the red giant is shown in Table 3, and the non-standard TRGB model shows the, now typical, differences in bolometric luminosity, radius and temperature. However, this time the fate of the exoplanet on the canonical scenario remains uncertain, as the orbit does not decrease fast enough to become engulfed within the red giant before the helium flash (requiring a more detailed model to estimate if the planet would spiral down towards the stellar core). This is not the case for the non-standard scenario in which the enhanced cooling of the stellar core, along with the loss of orbital angular momentum caused by tidal drag, appears to accelerate the stellar expansion fast enough for the stellar radius to reach the orbit of the planet.

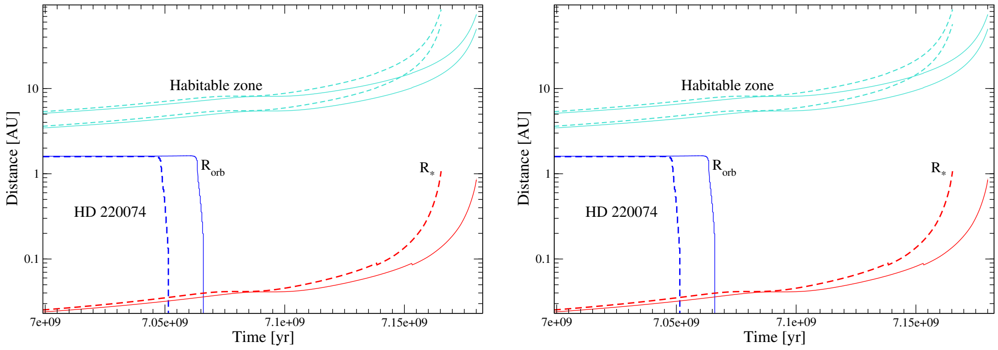

Fig. 1. Temporal evolution, in the HD 220074 (left panel) and HD 158996 (right) stellar systems, of R_{orb} (dark blue lines), R_* (red) and the inner and outer limits of the habitable zone (light blue), in the canonical (solid) and non-standard (dashed) scenarios.

Table 2. Best fitting stellar models for the star HD 220074 (now) and for its TRGB in the canonical and non-standard scenarios.

	Now	Canonical	Non-std.
M_* [$M_\odot$]	1.20	1.049	1.049
L_{bol} [$L_\odot$]	374	2601	3489
R_* [$R_\odot$]	42	180	233
T_{eff} [K]	3939	3073	2910

Table 3. Best fitting stellar models for the star HD 158996 (now) and for its TRGB in the canonical and non-standard scenarios.

	Now	Canonical	Non-std.
M_* [$M_\odot$]	1.80	1.736	1.735
L_{bol} [$L_\odot$]	374	2485	3495
R_* [$R_\odot$]	42	143	183
T_{eff} [K]	4100	3408	3280

4. Conclusions

The simultaneous emission of axions and neutrinos, whose production rate is enhanced by the non-standard decay of plasmons due to a non-zero magnetic dipole moment, augments the radius and luminosity of low-mass red giants. As with the solar case, bolometric luminosity increases by around a thousand times the solar value (depending on the specific values for initial mass and chemical composition). The increment in bolometric luminosity is a direct result of the increment in the mass of the degenerate core (reaching to about 0.048 $M_\odot$ for the stellar track with M_i = 1.9 $M_\odot$ and Z_i = 0.02). In this respect, the evidence from the photometric calibrations of the TRGB of globular clusters will be revisited by considering the simultaneous production of axions and neutrinos (this could help to get even smaller constraints on the axion-electron coupling constant and the magnetic dipole moment for neutrinos. On the exoplanet side, the increment in bolometric luminosity just before the helium flash pushes the limit of the habitable zone outwards, this could be important for Earth-like exoplanets within this kind of stellar systems. Also, the accelerated expansion rate appears to dramatically increase the tidal drag, inducing a larger probability that any exoplanet, orbiting close enough, could become engulfed by the stellar photosphere even if the star does not grow to a size comparable to the orbital distance of the planet. However, more precise orbital models need to be calculate in order to study this matter any further.

Acknowledgements. I am grateful towards Dr. Klaus-Peter Schröder, for all the interesting discussions and for always serving as a guide and as a good friend; to Dr. Miguel Chavez for his kind invitation to participate as a speaker in the conference and to MC. Saturnino Castro Reyes for always supporting my professional development and my participation in Academic Conferences.

References

Arceo-Díaz, S., et al. 2015, Astroparticle Physics, 70, 1
Arceo-Díaz, S., et al. 2015, RMxAA, 51, 151
Arceo-Díaz, S., et al. 2019, Journal of Physics Conf. Ser., 1160, 012007
Bang, T. Y., et al. 2018, Journal of Korean Astronomical Society, 51, 17
Eggleton, P. 1971, MNRAS, 151, 351
Haft, M., Raffelt, G. G., & Weiss, A. 1994, ApJ, 425, 222
Itoh, N., et al. 1992, ApJ, 395, 622
Itoh, N., et al. 1996, ApJS, 102, 411
Jiang, J. H., & Zhu, S. 2018, Research Notes of the American Society, 2, 185
Lee, B. C., Han, I., & Park, M. G. 2013, A&A, 549, A2
Pols, O. R., Tout, C. A. & Eggleton, P. P. 1995, MNRAS, 274, 964
Raffelt, G. G. & Weiss, A. 1992, A&A, 264, 536
Raffelt, G. G., & Weiss, A. 1995, Phys. Rev. D, 51, 1495
Ramírez, R. M., & Kaltenegger, L. 2016, ApJ, 823, 14
Schröder, K. P., & Cuntz, M. 2005, ApJ, 630, 1
Schröder, K. P., & Smith, C. 2008, MNRAS, 386, 155
Whitmire, D., & Reynolds, R., 1996, in Circumstellar Habitable Zones, L. R. Doyle ed. (Travis House, Menlo Park, CA), 117
Zahn, J. P. 1977, A&A, 57, 383